

Master equation approach to DNA breathing in heteropolymer DNA

Tobias Ambjörnsson,^{1,*} Suman K. Banik,² Michael A. Lomholt,^{1,†} and Ralf Metzler^{1,‡}

¹NORDITA (*Nordic Institute for Theoretical Physics*), Blegdamsvej 17, DK-2100 Copenhagen Ø, Denmark

²Department of Physics, Virginia Polytechnic Institute and State University, Blacksburg, Virginia 24061-0435, USA

(Received 19 October 2006; published 16 February 2007)

After crossing an initial barrier to break the first base-pair (bp) in double-stranded DNA, the disruption of further bps is characterized by free energies up to a few $k_B T$. Thermal motion within the DNA double strand therefore causes the opening of intermittent single-stranded denaturation zones, the DNA bubbles. The unzipping and zipping dynamics of bps at the two zipper forks of a bubble, where the single strand of the denatured zone joins the still intact double strand, can be monitored by single molecule fluorescence or NMR methods. We here establish a dynamic description of this DNA breathing in a heteropolymer DNA with given sequence in terms of a master equation that governs the time evolution of the joint probability distribution for the bubble size and position along the sequence. The transfer coefficients are based on the Poland-Scheraga free energy model. We derive the autocorrelation function for the bubble dynamics and the associated relaxation time spectrum. In particular, we show how one can obtain the probability densities of individual bubble lifetimes and of the waiting times between successive bubble events from the master equation. A comparison to results of a stochastic Gillespie simulation shows excellent agreement.

DOI: 10.1103/PhysRevE.75.021908

PACS number(s): 87.15.-v, 05.40.-a, 82.37.-j, 02.50.-r

I. INTRODUCTION

DNA is made up of the four bases A (adenine), C (cytosine), G (guanine) and T (thymine), that form the Watson-Crick base pairs (bps) AT and GC according to the key-lock principle. Under normal temperatures and salt conditions, DNA assumes the double-helical B configuration. The double helix is the thermodynamically stable state of DNA in a wide range of temperature and salt conditions [1,2]. Measured through changes of UV absorption and small-angle neutron scattering in DNA solutions, a gradual denaturation of the DNA double strand is observed by increasing the temperature, or by titration with acid or alkali. During melting, the stability of the DNA duplex is related to the content of GC base pairs: the larger the fraction of GC bps, the higher the required melting temperature or pH value. Thus under melting, double-stranded DNA starts to unwind in regions rich in AT bps, and then proceeds to regions of progressively higher GC content [1,2]. The single-stranded domains formed during the melting of the double strand are called DNA bubbles. Their size increases from a few broken base pairs to a few hundred open bps just below the melting temperature T_m . Eventually, a transition occurs to full denaturation at T_m , and the two DNA single strands are completely separated [1–4]. Cycling of DNA melting and subsequent recombination of the denatured single strand in a solution containing single bases is used to produce large numbers of copies of the ori-

nal DNA sequence in the polymerase chain reaction (PCR) [5]. Apart from denaturation by melting or titration, individual DNA molecules can be mechanically denatured by use of optical traps: Attaching each end of a single, linear stretch of DNA to small dielectric beads, a longitudinal tension along the double-strand can be induced by pulling on the beads, until around 65 pN when a force plateau is reached. This plateau corresponds to the denaturation transition [6,7]. Together with DNA superstructure and DNA knots, DNA bubbles are currently receiving high interest as examples of the relevance of local and global DNA conformations to the function of DNA [8,9].

DNA stability is effected by the combination of the free energies ϵ_{hb} for breaking a Watson-Crick hydrogen bond between complementary AT and GC bases in a single bp (transversal interactions), and the ten independent (longitudinal) stacking free energies ϵ_{st} for disrupting the interactions between a nearest neighbor pair of bps. At 100 mM NaCl concentration and $T=37$ °C the hydrogen bonding amounts to $\epsilon_{hb}=1.0k_B T$ for a single AT and $0.2k_B T$ for a GC bond [10]. The weakest (strongest) stacking energies were found to be the TA/AT (GC/GC) pair with free energies $\epsilon_{st}=-0.9k_B T$ ($-4.1k_B T$) [11]. Note that negative values for the free energies denote stable states. Thus the overall free energy cost of breaking a GC bp, that is paired with an intact CG bp downstream of the DNA sequence and whose nearest neighbor bp upstream is already denatured, is $-3.9k_B T$. In contrast, breaking an AT bp next to a TA is marginally unstable with a free energy release on bp disruption of $0.1k_B T$. The relatively small free energies ϵ_{st} for base stacking stem from the fact that relatively large amounts of binding enthalpy (of the order of $12k_B T$ at 37 °C) on the one hand, and entropy release on breaking the stacking interactions and Watson-Crick bonds on the other hand, almost cancel.

This cancellation effect does not hold for the breaking of the first bp that acts as a seed for a new bubble. Roughly speaking, the bubble initiation is characterized by the break-

*Present address: Department of Chemistry, Massachusetts Institute of Technology, 77 Massachusetts Avenue, Cambridge, MA 02139, USA. Electronic address: ambjorn@mit.edu

†Present address: Department of Physics, University of Ottawa, 150 Louis Pasteur, Ottawa, Ontario, Canada K1N 6N5.

‡Present address: Department of Physics, University of Ottawa, 150 Louis Pasteur, Ottawa, Ontario, Canada K1N 6N5. Electronic address: metz@nordita.dk

ing of two stacking interactions when the first bp is disrupted; the accompanying enthalpy cost cannot be balanced by the entropy gain of the two, still strongly confined, liberated bases. Thus the creation of two boundaries between the intact double-helix and the bubble nucleus is associated with an activation cost of some 7 to 12 $k_B T$, corresponding to the Boltzmann weight $\sigma_0 \approx 10^{-3} \cdots 10^{-5}$ [3,4,12,13]. Note that this cooperativity parameter σ_0 is related to the ring-factor ξ used in [11,14], see below. The high bubble initiation barrier guarantees the stability of DNA at physiological conditions. It also makes sure that, below T_m , individual bubbles are well-separated from each other along the sequence and can be considered to be statistically independent.

Already at room temperature, DNA bubbles form spontaneously due to thermal unzipping of bps. Due to the relatively high free energy barrier represented by the cooperativity factor σ_0 , such bubble events are rare. However, once this barrier is overcome, the unzipping of further bps occurs at relatively low free energy costs (see above discussion). DNA bubbles have thus been successfully observed by NMR techniques [15] and, more recently, by single molecule fluorescence correlation methods revealing a bubble lifetime of up to a few ms, and pronouncedly multistate kinetics [16]. The latter characterizes the stepwise unzipping and zipping of bps. The accompanying stepwise motion of the two zipper forks (where the still intact double strand meets the two single strands of the denaturation domain) of a DNA bubble corresponds to a random walk along the bp sequence. Below T_m , this random walk is biased toward bubble closure.

At this point, a remark on the relevance of DNA breathing for the biological function of DNA is in order. In the intact double-helix, the nucleobases are shielded from damage to preserve the genetic code. This, however, also means that the reactive groups of the nucleobases are buried inside the double helix. The interaction with specific chemicals, binding proteins, or enzymes with DNA requires the accessibility of the reactive groups of the bases. This access is provided by the formation of DNA bubbles. Thus, albeit infrequent, the formation of intermittent DNA bubbles via DNA breathing is crucial for the function of DNA. Apart from the binding of passive (no energy consumption from, e.g., ATP hydrolysis) chemicals or binding proteins, even the initiation of transcription through polymerase has been implicated to be facilitated by DNA bubbles [17,18]. When selectively single-stranded DNA binding proteins (SSBs) attempt to attach to fluctuating DNA bubbles, a competition occurs between the time scales characterizing protein (un)binding and bubble (un)zipping. For biological systems, the SSB binding is kinetically suppressed by the comparatively fast bubble dynamics, while for certain SSB mutants the protein binding lowers the mechanical melting force, and may lead to full SSB-binding-induced DNA denaturation [19–23].

A considerable amount of work has been dedicated to the equilibrium and dynamical modeling of DNA denaturation. The stacking and hydrogen bonding free energies are used to construct the partition function of the statistical mechanical Poland-Scheraga model [3,11]. Interpreting DNA breathing as a random walk process in the Poland-Scheraga free energy landscape, DNA bubble dynamics has been modeled in terms of a Fokker-Planck equation approach [24]. By mapping this

continuum approach onto the imaginary time Schrödinger equation of the quantum Coulomb problem, the dynamic exponents of the bubble lifetime distribution and correlation function were derived recently [25], generalizing previous results from Ref. [26]. The coalescence time distribution of two bubbles on a DNA construct was obtained in a vicious walker model [27]. A master equation approach mirroring the discrete nature of the bp structure developed in Refs. [22,23] was generalized to an arbitrary sequence of bps in Refs. [18,28]. This latter model was demonstrated to reproduce well the autocorrelation function measured in the above mentioned single molecule fluorescence experiments [16]. A stochastic simulation scheme corresponding to the master equation approach was developed in Ref. [29]. The influence of a Gaussian random energy landscape on bubble localization and dynamics was studied in Ref. [30]. Apart from approaches based on the Poland-Scheraga model, DNA breathing has been investigated on the bases of the more microscopically oriented Peyrard-Bishop model [31,32].

In this paper we investigate a (2+1)-variable master equation that governs the time evolution of the probability distribution $P(x_L, m, t)$ to find a bubble consisting of m broken bps with left and right fork positions x_L and $x_R = x_L + m + 1$ along the sequence. With this approach an arbitrary DNA sequence can be analyzed and its breathing behavior predicted. We discuss the exact form of the transfer matrix containing the rate coefficients for all permitted jumps and derive the bubble autocorrelation function with associated relaxation time spectrum. To be able to connect to the time series obtained from the complementary stochastic simulation, we derive the probability densities for the bubble lifetime and the waiting times between successive bubble events. Finally, we show that in the homopolymer limit, analytical results can be obtained.

II. ONE-BUBBLE PARTITION FUNCTION AND TRANSFER COEFFICIENTS

Below the melting temperature T_m , a single bubble can be considered to be statistically independent due to the high nucleation barrier for initiating a bubble quantified by $\sigma_0 \ll 1$ [23], such that opening and merging of multiple bubbles are rare, and a one-bubble picture is appropriate. In the particular case of the bubble constructs used in the fluorescence correlation experiments of Ref. [16], the sequence is designed such that there is a single bubble domain. Referring to these constructs, we consider a segment of double-stranded DNA with M internal bps. These bps are clamped at both ends such that the bps $x=0$ and $x=M+1$ are always closed (Fig. 1). The sequence of bps determines the Boltzmann weights $u_{hb}(x) = \exp\{\epsilon_{hb}(x)/(k_B T)\}$ for Watson-Crick hydrogen bonding at position x , and the Boltzmann factor $u_{st}(x) = \exp\{\epsilon_{st}(x)/(k_B T)\}$ for pure bp-bp stacking between bps $x-1$ and x , respectively. In the bubble domain, the left and right zipper fork positions x_L and x_R denoting the right- and leftmost closed bp of the bubble are stochastic quantities, whose random motion underlies the bubble dynamics.

Instead of using the fork positions x_L and x_R , we prefer to work with the left fork position x_L and the bubble size m

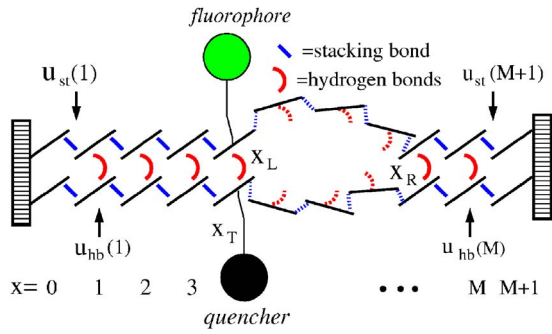


FIG. 1. (Color online) Clamped DNA domain with internal bps $x=1$ to M , statistical weights $u_{\text{hb}}(x)$, $u_{\text{st}}(x)$, and tag position x_T . The DNA sequence enters through the statistical weights $u_{\text{st}}(x)$ and $u_{\text{hb}}(x)$ for disrupting stacking and hydrogen bonds, respectively. The bubble breathing process consists of the initiation of a bubble and the subsequent motion of the forks at positions x_L and x_R , see also Fig. 2.

$=x_R-x_L-1$. For these variables, the partition function of the bubble becomes

$$\mathcal{Z}(x_L, m) = \frac{\xi'}{(1+m)^c} \prod_{x=x_L+1}^{x_L+m} u_{\text{hb}}(x) \prod_{x=x_L+1}^{x_L+m+1} u_{\text{st}}(x) \quad (1)$$

for $m \geq 1$. At $m=0$, we define $\mathcal{Z}(m=0)=1$. In relation (1), instead of the usual cooperativity parameter σ_0 we use the factor $\xi' = 2^c \xi$ related to the ring factor $\xi \approx 10^{-3}$ introduced in Ref. [11]. For a homopolymer, this ξ is related to σ_0 by $\sigma_0 = \xi \exp\{\epsilon_{\text{st}}/(k_B T)\}$ [11]. The denominator in Eq. (1) represents the entropy loss on formation of a closed polymer loop, where the offset by one accounts for finite size effects [12,33]. The associated critical exponent is $c=1.76$ [34]. For a given bubble size, the partition (1) counts m contributions from broken hydrogen bonds and $m+1$ from disrupted stack-

ing interactions. The partition (1) defines the equilibrium probability

$$P^{\text{eq}}(x_L, m) = \frac{\mathcal{Z}(x_L, m)}{\sum_{m=1}^M \sum_{x_L=0}^m \mathcal{Z}(x_L, m)} \quad (2)$$

for finding a bubble of size m at location x_L .

The zipping and unzipping of individual bps was found to occur on time scales of the order of tens of μs [16]. In comparison, the polymeric degrees of freedom of a bubble equilibrate much faster, and therefore the positions x_L and x_R of the two zipper forks (or, equivalently, x_L and the bubble size $m=x_R-x_L-1$) are the slow variables of the system. We use them as dynamic variables to characterize the bubble dynamics. The faster polymeric degrees of freedom of the relatively small bubble enter effectively through the partition (1). Moreover, it was shown that the time scale of bp zipping and unzipping follows an Arrhenius behavior [16], corresponding to a barrier crossing picture of the zipper motion. It therefore seems reasonable to assume that the bubble is close to equilibrium. Under this assumption, the partition (1) defines the transition probabilities between different states. These conditions allow us to introduce the master equation (9) with its transfer matrix \mathcal{W} below. To introduce the underlying time scales, we first define the transfer coefficients.

The allowed transitions with the associated transfer (rate) coefficients are sketched in Fig. 2. The left zipper fork is characterized by the rate $t_L^+(x_L, m)$ corresponding to the process $x_L \rightarrow x_L+1$ of bubble size decrease, and $t_L^-(x_L, m)$ for $x_L \rightarrow x_L-1$ (bubble size increase). Similarly, we introduce $t_R^+(x_R, m)$ for $x_R \rightarrow x_R+1$ (bubble size increase) and $t_R^-(x_R, m)$ for $x_R \rightarrow x_R-1$ (decrease). These rates are valid for transitions between states with $m \geq 1$. Bubble opening (initiation) $m=0 \rightarrow m=1$ is quantified by $t_G^+(x_L)$, and bubble closing (an-

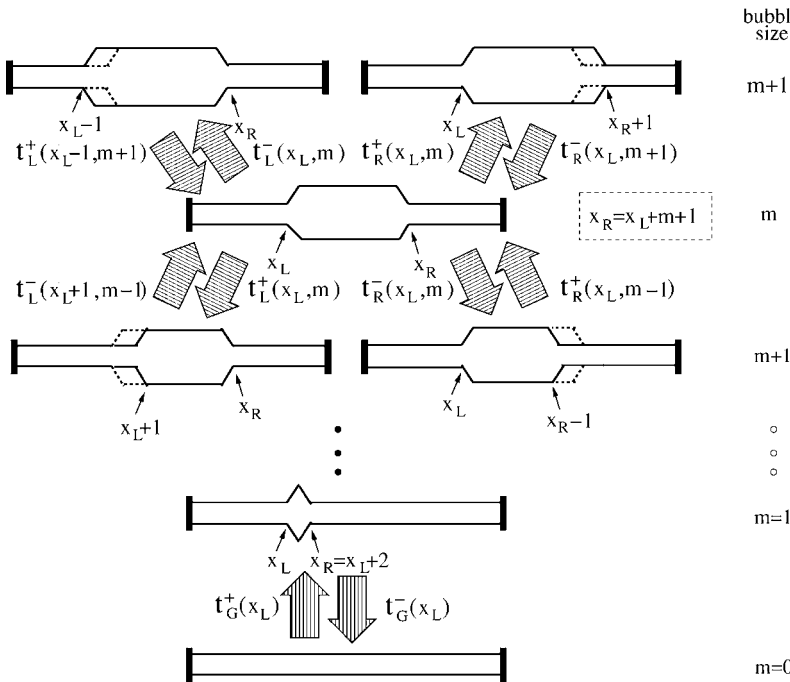


FIG. 2. Possible bubble (un)zipping transitions: for $m \geq 2$, the four transfer rates $t_{L/R}^\pm(x_L, m)$ completely determine the transitions *out of* this state; the coefficients $t_L^\pm(x_L \mp 1, m \pm 1)$ and $t_R^\pm(x_R \mp 1, m \pm 1)$ specify the possible jumps *into* this state. Jumps between state $m=1$ and ground state $m=0$ are described by $t_G^+(x_L)$ and $t_G^-(x_L)$.

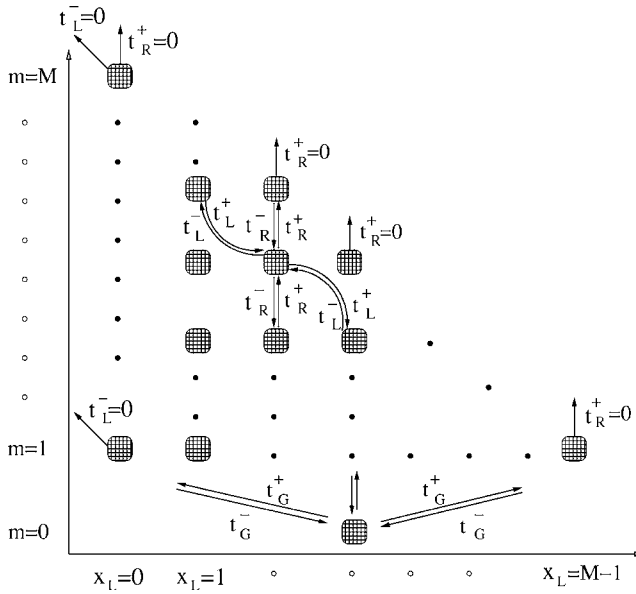


FIG. 3. Schematic representation of the (x_L, m) -lattice on which the DNA-bubble jump process takes place, with the permitted transitions; compare to Figs. 1 and 2. The boundary conditions Eq. (3) are also indicated. For $m \geq 1$ jumps are determined by the rates $t_{L/R}^\pm$. A jump between the ground state $m=0$ and one of the $m=1$ states occurs with rates t_G^\pm . Note that the ground state $m=0$ is unique; from the ground state, a bubble can be initiated at any point in the row $m=1$, with the appropriate weight $t_G^+(x_L)$. Note that all allowed jumps correspond to a change in bubble size m , i.e., there are no allowed “horizontal” transitions in the (x_L, m) -lattice.

nihilation) by $m=1 \rightarrow 0$ by $t_G^-(x_L)$. Note that by our definitions $t_G^+(x_L)$ and $t_G^-(x_L)$ actually correspond to bubble opening/closing at $x=x_L+1$. Clamping requires that $x_L \geq 0$ and $x_R \leq M+1$, corresponding to the reflecting boundary conditions [35]

$$t_L^-(x_L=0, m) = t_R^+(x_L, m=M-x_L) = 0. \quad (3)$$

In Fig. 3 we sketch schematically the allowed transitions in the m - x_L plane.

In order to define the various transfer rates t , we first impose the detailed balance conditions (compare [36,37])

$$\frac{t_L^+(x_L-1, m+1)}{t_L^-(x_L, m)} = \frac{P_{\text{eq}}(x_L, m)}{P_{\text{eq}}(x_L-1, m+1)}, \quad (4a)$$

$$\frac{t_R^-(x_L, m+1)}{t_R^+(x_L, m)} = \frac{P_{\text{eq}}(x_L, m)}{P_{\text{eq}}(x_L, m+1)}, \quad (4b)$$

$$\frac{t_G^+(x_L)}{t_G^-(x_L)} = \frac{P_{\text{eq}}(x_L, 1)}{P_{\text{eq}}(0)}, \quad (4c)$$

that ensure relaxation toward the equilibrium distribution $P^{\text{eq}}(x_L, m)$, see Eq. (2). The detailed balance conditions do not uniquely define the transfer rates t , leaving a certain freedom of choice [37]. We use the following conventions.

To define the zipping rate, we assume that it is independent of the position x along the DNA sequence. The picture behind is that the closure of the bp is dominated by the requirement that the two bases diffuse in real space until mutual encounter and eventual bond formation. As sterically AT and GC bps are very similar, the zipping rate should not significantly vary with the individual nature of the involved bps, and we choose the constant rate $k/2$, see below. The rate constant k is the only adjustable parameter of our model and has to be independently determined from experiment or more fundamental models. Our choice for the zipping rate is not unique. Instead, an x -dependence of k could easily be introduced by selecting different powers of the statistical weights entering the rate coefficients for zipping and unzipping, such that they still fulfill detailed balance, compare Ref. [37]. According to this, a decrease in bubble size due to zipping of the bp closest to either the left or the right zipper fork is therefore ruled by

$$t_L^+(x_L, m)|_{m \geq 2} = t_R^-(x_L, m)|_{m \geq 2} = \frac{k}{2}, \quad (5)$$

respectively. Note that the factor 1/2 is introduced for consistency with previous approaches [22,23]. Note also that for simplicity we do not introduce the hook exponent discussed in previous studies [18,23,28]. This exponent should be important for large bubbles, when during the zipping process not only the bp at the zipper fork is moved, but also part of the vicinal single strand dragged or pushed along [23,28,38].

According to the detailed balance condition and Eq. (5), increase in bubble size is controlled by

$$t_L^-(x_L, m) = \frac{k}{2} u_{\text{st}}(x_L) u_{\text{hb}}(x_L) s(m), \quad (6a)$$

$$t_R^+(x_L, m) = \frac{k}{2} u_{\text{st}}(x_R+1) u_{\text{hb}}(x_R) s(m), \quad (6b)$$

for $m \geq 1$, where

$$s(m) = \left(\frac{1+m}{2+m} \right)^c. \quad (7)$$

For $m \geq 1$ we thus take the bubble increase rate coefficients proportional to the first power of the Arrhenius factor $u_{\text{st}} u_{\text{hb}} = \exp\{(\epsilon_{\text{hb}} + \epsilon_{\text{st}})/[k_B T]\}$ times the loop correction $s(m)$. We stress that Eqs. (6a) and (6b) are dictated by the detailed balance condition, once the convention (5) is established. As noted, detailed balance would still be fulfilled, for instance, if only a fractional power α^q of the Arrhenius factor α appeared in the opening rates if complemented by the respective power α^{q-1} in the closing rates.

Finally, we define

$$t_G^+(x_L) = k \xi' s(0) u_{\text{st}}(x_L+1) u_{\text{hb}}(x_L+1) u_{\text{st}}(x_L+2), \quad (8a)$$

$$t_G^-(x_L) = k \quad (8b)$$

for bubble initiation and annihilation from and to the zero-bubble state $m=0$, with the bubble initiation factor ξ' in the expression for t_G^+ . As bubble initiation involves breaking of

two stacking interactions at consecutive bps, we have the factor $u_{st}(x_L+1)u_{st}(x_L+2)$ in expression (8a). The last open bp can zip close from either side, so the bubble closing rate $t_G^-(x_L)$ makes up twice the zipping rate of a single fork.

The rates t together with the boundary conditions fully determine the bubble dynamics. In the next section, we establish the master equation for the time evolution of the distribution $P(m, x_L, t)$ and derive the associated quantities.

III. MASTER EQUATION FOR DNA BREATHING

The joint probability distribution $P(t) = P(x_L, m, t; x'_L, m', 0)$ measures the likelihood that at time t the system is in state $\{x_L, m\}$ and that at $t=0$ it was in state $\{x'_L, m'\}$. Its time evolution is controlled by the master equation

$$\frac{\partial}{\partial t} P(t) = \mathcal{W}P(t). \quad (9)$$

The explicit form of the transfer matrix \mathcal{W} is discussed in detail in Sec. IV. Here, we concentrate on how to derive the quantities relevant for the description of DNA-breathing experiments. In that course we introduce the eigenmode ansatz [36,37]

$$P(t) = \sum_p c_p Q_p \exp(-\eta_p t), \quad (10)$$

where the coefficients c_p are fixed by the initial condition. Combining Eqs. (10) and (9), the eigenvalue equation

$$\mathcal{W}Q_p = -\eta_p Q_p \quad (11)$$

yields, compare Ref. [37] and below for more details. The eigenvalues η_p and eigenvectors Q_p allow one to compute any quantity of interest. In fact, the autocorrelation function for bubble breathing and the corresponding relaxation time distribution are quite straightforward to obtain, see Sec. III A. Below, in Sec. III B, we discuss the more subtle point how the probability densities for the bubble lifetime and the interbubble event waiting time can be derived.

A. Blinking autocorrelation function of a tagged bp

Motivated by the fluorescence correlation setup in Ref. [16] we are interested in the state of a tagged bp at $x=x_T$, see Fig. 1. In the experiment fluorescence occurs if the bps in a Δ -neighborhood of the fluorophore position x_T are open [16]. Measured fluorescence blinking time series thus correspond to the stochastic variable $I(t)$, defined by

$$I(t) = \begin{cases} 1, & \text{if at least all bps in } [x_T - \Delta, x_T + \Delta] \text{ open} \\ 0, & \text{otherwise.} \end{cases} \quad (12)$$

The stochastic variable is therefore $I=1$ if the system is in the region

$$\mathbb{R}1: \{0 \leq x_L \leq x_T - \Delta - 1, x_T - x_L + \Delta \leq m \leq M - x_L\} \quad (13)$$

of the phase space spanned by x_L and m . Conversely, $I=0$ corresponds to the complement set $\mathbb{R}0$.

The equilibrium autocorrelation function of fluorescence blinking is defined by

$$A(x_T, t) = \langle I(t)I(0) \rangle - \langle \langle I \rangle \rangle^2, \quad (14)$$

where the angles $\langle \cdot \rangle$ denote an ensemble average over the equilibrium distribution P_{eq} . $A(x_T, t)$ quantifies the relaxation dynamics of the tagged bp. This is evident from the identity

$$\langle I(t)I(0) \rangle = \sum_{I=0}^1 \sum_{I'=0}^1 I \rho(I, t; I', 0) I' = \rho(1, t; 1, 0), \quad (15)$$

where $\rho(1, t; 1, 0)$ is the survival probability that $I(t)=1$ and that $I(0)=1$. From the definition of the two regions $\mathbb{R}1$ and $\mathbb{R}0$ it follows that $\rho(1, t; 1, 0)$ yields from summation of $P(x_L, m, t; x'_L, m', 0)$ solely over region $\mathbb{R}1$:

$$\rho(1, t; 1, 0) = \sum_{x_L, m, x'_L, m' \in \mathbb{R}1} P(x_L, m, t; x'_L, m', 0). \quad (16)$$

Together with Eq. (15), combined with the eigenmode decomposition (10), and under the assumption that initially the system is at equilibrium, we obtain

$$P(x_L, m, 0; x'_L, m', 0) = \delta_{mm'} \delta_{x_L x'_L} P_{eq}(x_L, m), \quad (17)$$

such that we can rewrite the autocorrelation function (14) in the form

$$A(x_T, t) = \sum_{p \neq 0} [T_p(x_T)]^2 \exp(-t/\tau_p). \quad (18)$$

Here, we use the relaxation times $\tau_p = 1/\eta_p$, and abbreviate

$$T_p(x_T) = \sum_{x_L=0}^{x_T-\Delta-1} \sum_{m=x_T-x_L+\Delta}^{M-x_L} Q_p(x_L, m). \quad (19)$$

In all illustrations, we plot the normalized form of the autocorrelation function, $A(x_T, t)/A(x_T, 0) = A(x_T, t)/[\sum T_p(x_T)]^2$.

The autocorrelation function $A(x_T, t)$ can be rewritten as the integral $A(x_T, t) = \int d\tau \exp(-t/\tau) f(x_T, \tau)$ defining the weighted spectral density (relaxation time spectrum)

$$f(x_T, \tau) = \sum_{p \neq 0} [T_p(x_T)]^2 \delta(\tau - \tau_p). \quad (20)$$

This quantity indicates how many different exponential modes contribute to the autocorrelation function. If $f(x_T, \tau)$ is very narrow, the process is approximately exponential, whereas a broad relaxation time spectrum indicates that many different modes play together. While close to T_m the relaxation time spectrum becomes dominated by the longest relaxation mode, at lower T the spectrum is typically broad [23].

B. Survival and waiting time densities of a tagged bp

The autocorrelation function $A(x_T, t)$ is an equilibrium average measure for a single bubble. It does not contain any information on the distribution of the lifetimes of individual bubbles or the waiting time elapsing between annihilation of one bubble and initiation of the next. This information is

provided by the survival time and waiting time densities $\phi(t)$ and $\psi(t)$ derived here.

Survival time and waiting time densities correspond to a first passage problem to, respectively, start from an initial state with $I(0)=1$ or $I(0)=0$, and transit to a state $I(t)=0$ or $I(t)=1$ after time t . To obtain these quantities from the master equation framework, one needs to solve the reduced eigenvalue problem [37]

$$\mathcal{W}\bar{Q}_p = -\bar{\eta}_p\bar{Q}_p \quad (21)$$

for coordinates belonging to R1 and R0. Details are collected in Sec. IV. The reduced eigenvalue *Ansätze* (21) for R1 and R0 possess only positive eigenvalues, $\bar{\eta}_p > 0$ for all p . This reflects the fact that there exist transitions from one region to the other, such that probability “leaks out.” In terms of the reduced eigenvalues $\bar{\eta}_p$ and eigenvectors \bar{Q}_p the survival and waiting time densities become

$$\psi(t) = \sum_{p \in R0} \bar{\eta}_p \bar{c}_p \exp(-\bar{\eta}_p t), \quad (22a)$$

$$\phi(t) = \sum_{p \in R1} \bar{\eta}_p \bar{c}_p \exp(-\bar{\eta}_p t) \quad (22b)$$

with the coefficients

$$\bar{c}_p = \frac{\bar{\eta}_p \left[\sum_{x_L, m} \bar{Q}_p(x_L, m) \right]^2}{\sum_p \bar{\eta}_p \left[\sum_{x_L, m} \bar{Q}_p(x_L, m) \right]^2}. \quad (22c)$$

The sums over m, x_L are restricted to regions R1 and R0 for the survival and waiting time densities, respectively. Both survival and waiting time probability densities are normalized, $\int \psi(t) dt = 1$ and $\int \phi(t) dt = 1$, since $\sum_p \bar{c}_p = 1$.

We point out that a nontrivial problem connected to obtaining the appropriate expressions for $\psi(t)$ and $\phi(t)$ is how to choose the right initial distribution of states (there are many states corresponding to a bubble being just open/closed). We chose an initial distribution determined by the distribution of stationary flux into the regions R1 and R0. This choice guarantees that (for long times) the ratio of the time spent in the $I=1$ state versus the time spent in the $I=0$ state is given by the equilibrium results as required by ergodicity, see Sec. IV for details.

In the Appendix we briefly discuss how stochastic modeling can be used to obtain single bubble time series, from which all quantities such as the fluorescence blinking autocorrelation function, as well as the survival and waiting time densities, can be distilled. Both approaches converge nicely [18,28].

IV. MASTER EQUATION: THE DETAILS

In this section we show the explicit form for the master equation with its transfer matrix \mathcal{W} and go into details of how to solve it numerically. We also present details of the formalism to derive the waiting and survival densities $\psi(t)$ and $\phi(t)$.

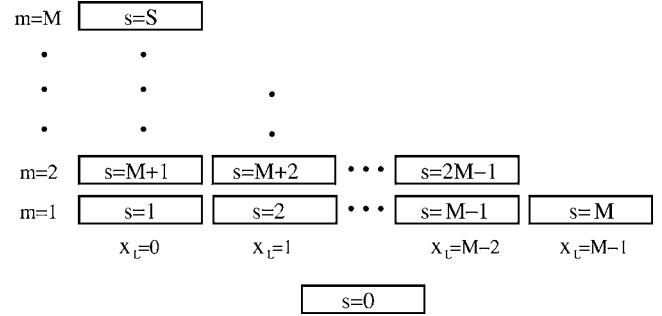


FIG. 4. Enumeration scheme for the numerical analysis: The two-dimensional grid points (x_L, m) are replaced by a one-dimensional running variable s . See text for details.

A. The \mathcal{W} -matrix

In order to present an explicit expression for the \mathcal{W} -matrix in Eqs. (9) and (11) it is convenient to replace the two-dimensional grid points (x_L, m) by a one-dimensional coordinate s counting all lattice points, compare [23]. We choose the enumeration illustrated in Fig. 4.

From this figure we notice that $m \in [0, M]$ and $x_L \in [0, M-m]$. We label the ground state $m=0$ by $s=0$. For $m \geq 1$ an arbitrary s -point can be obtained from a specific (x_L, m) according to

$$s = s|_{x_L}^m = (m-1)M - \frac{(m-1)(m-2)}{2} + x_L + 1. \quad (23)$$

From this relation we notice that the maximum s value is

$$S = \max\{s\} = \frac{M(M+1)}{2}, \quad (24)$$

i.e., the size of the relevant \mathcal{W} -matrix (see below) scales as M^2 . Expression (23) allows us to change the dependence of the transfer coefficients to the s -variable, $t_{L/R}^\pm(x_L, m) \rightarrow t_{L/R}^\pm(s)$, using the explicit expressions (5), (6a), and (6b) for the transfer coefficients, together with the boundary conditions in Eqs. (3). Also $t_G^\pm(x_L, m) \rightarrow t_G^\pm(s)$, following Eqs. (8a) and (8b). From Eq. (23) and Fig. 4 we notice that

$$\begin{aligned} s|_{x_L=1}^{m+1} &= s|_{x_L}^m + M - m, \quad \text{for } x_L \geq 1 \text{ and } m \leq M-1, \\ s|_{x_L=1}^{m-1} &= s|_{x_L}^m - (M - m + 1), \quad \text{for } m \geq 2, \\ s|_{x_L}^{m-1} &= s|_{x_L}^m - (M - m + 2), \quad \text{for } m \geq 2, \\ s|_{x_L}^{m+1} &= s|_{x_L}^m + M - m + 1, \quad \text{for } x_L \leq M - (m+1) \text{ and} \\ &\quad m \leq M-1. \end{aligned} \quad (25)$$

We can then write Eq. (11) explicitly as

$$\sum_{s'} \mathcal{W}(s, s') Q_p(s') = -\eta_p Q_p(s), \quad (26)$$

where the matrix elements are

$$\mathcal{W}(s, s + M - m) = t_L^+(s + M - m), \quad \text{for } s \cap x_L \geq 1 \text{ and } m > 1,$$

$$\begin{aligned}
\mathcal{W}(s, s - [M - m + 1]) &= t_L^-(s - [M - m + 1]), \quad \text{for } s \cap m \geq 2, \\
\mathcal{W}(s, s - [M - m + 2]) &= t_R^+(s - [M - m + 2]), \quad \text{for } s \cap m \geq 2, \\
\mathcal{W}(s, s + M - m + 1) &= t_R^-(s + M - m + 1), \text{ for } s \cap x_L \leq M - (m \\
&\quad + 1), \quad \text{and } 1 \leq m \leq M - 1, \\
\mathcal{W}(s, s) &= -[t_L^+(s) + t_L^-(s) + t_R^+(s) + t_R^-(s)], \quad \text{for } sm \geq 2.
\end{aligned} \tag{27}$$

We have introduced the notation $s \cap$ with the meaning “ s is to be taken for x_L and m fulfilling” The positive terms above correspond to jumps *to* the state $\{x_L, m\}$, while the negative terms correspond to jumps *from* the state $\{x_L, m\}$, see Figs. 2 and 3. The probability for a bubble of size $m=1$ is altered by exchange with the $m=2$ state, or the $m=0$ ground state:

$$\mathcal{W}(0, x_L + 1) = t_G^+(x_L), \quad \text{for } s \cap m = 1,$$

$$\mathcal{W}(s, s) = -[t_G^-(x_L) + t_L^-(s) + t_R^+(s)], \quad \text{for } s \cap m = 1. \tag{28}$$

Finally, for the ground state population, we find

$$\mathcal{W}(0, x_L + 1) = t_G^-(x_L), \quad \text{for } x_L \leq M - 1,$$

$$\mathcal{W}(0, 0) = - \sum_{x_L=0}^{M-1} t_G^+(x_L), \tag{29}$$

i.e., the $m=0$ state can change by jumping to this state from $m=1$ (first term) or by jumping out of the $m=0$ state (second term). There are M possible jumps out from or to the ground state, corresponding to bubble opening or closing at any of the M internal bps. The remaining matrix elements are equal to zero. The problem at hand is that of determining the eigenvalues and eigenvectors of the $(S+1) \times (S+1)$ -matrix \mathcal{W} above. In terms of the running variable s , see Eq. (23), and the \mathcal{W} -matrix defined in Eqs. (27)–(29) the detailed balance conditions (4) can be written as

$$\mathcal{W}(s, s') P_{\text{eq}}(s') = \mathcal{W}(s', s) P_{\text{eq}}(s). \tag{30}$$

The eigenvectors are orthonormal in the sense [37]

$$\sum_s \frac{\mathcal{Q}_p(s) \mathcal{Q}_{p'}(s)}{P_{\text{eq}}(s)} = \delta_{p,p'}. \tag{31}$$

Convenient checks of the results of a numerical solution of the master equation then include: (i) there should be one zero eigenvalue $\eta_0=0$, the corresponding eigenvector is the equilibrium distribution, i.e., $\mathcal{Q}_0(s)=P^{\text{eq}}(s)$; (ii) the remaining eigenvalues should be real and negative (so that $\eta_p>0$ for $p \geq 1$); and (iii) the eigenvectors should satisfy the orthonormality relation, Eq. (31). Instead of working with the asymmetric matrix $\mathcal{W}(s, s')$, for numerical purposes it is sometimes preferable to use the symmetric matrix $\mathcal{V}(s, s') = \mathcal{Z}(s)^{-1/2} \mathcal{W}(s, s') \mathcal{Z}(s')^{1/2}$, see Refs. [37,39] for details. Indeed, the MATLAB code we used to numerically solve the master equation is based on the \mathcal{V} -matrix.

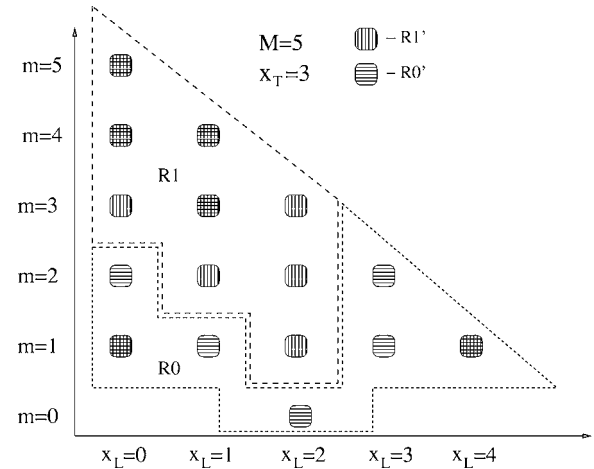


FIG. 5. Schematic of the (x_L, m) -points, region $R1$ ($R0$), for which the stochastic variable takes the value $I=1$ ($I=0$). The boundary points regions $R1'$ and $R0'$ are also indicated. The illustration is for the case $M=5$ and $x_T=3$, with $\Delta=0$.

B. Survival and waiting time densities

In this section we derive the expression for the waiting and survival time densities given in Eqs. (22). Denote by $\rho(t|s_{\text{init}})$ the first passage time density starting from some initial position $s_{\text{init}} \in R1'$ or $R0'$, see Fig. 5. The survival time density $\phi(t)$ and waiting time density $\psi(t)$ are then given by $\sum_{s_{\text{init}}} \rho(t|s_{\text{init}}) f(s_{\text{init}})$, where $f(s_{\text{init}})$ is the distribution of initial points in the region $R1'$ [for $\phi(t)$] or $R0'$ [for $\psi(t)$]. Following standard arguments (see, e.g., [40]) we can write the expression for $\rho(t|s_{\text{init}})$, and therefore $\psi(t)$ and $\phi(t)$, for which we find

$$\psi(t) = \sum_{p \in R0} \bar{\eta}_p \bar{c}_p \exp(-\bar{\eta}_p t), \tag{32a}$$

$$\phi(t) = \sum_{p \in R1} \bar{\eta}_p \bar{c}_p \exp(-\bar{\eta}_p t), \tag{32b}$$

where

$$\bar{c}_p = \sum_{s_{\text{init}}} \frac{\bar{Q}_p(s_{\text{init}}) f(s_{\text{init}})}{P_{\text{eq}}(s_{\text{init}})} \sum_s \bar{Q}_p(s). \tag{33}$$

Here, $s \in R0$ ($s \in R1$) for $\psi(t)$ [$\phi(t)$], and $\bar{\eta}_p$ and $\bar{Q}_p(s)$ are determined through the eigenvalue equation (21), which explicitly becomes in s -space [37]

$$\sum_{\tilde{s}} \mathcal{W}(s, \tilde{s}) \bar{Q}_p(\tilde{s}) = -\bar{\eta}_p \bar{Q}_p(s), \tag{34}$$

where $s, \tilde{s} \in R1$ when calculating the survival time density, and $s, \tilde{s} \in R0$ for the waiting time density.

The problem is now reduced to obtaining the distribution of initial points $f(s_{\text{init}})$ such that agreement with the Gillespie time series (see the Appendix) is obtained for long times. We define the rate coefficients for jumps from the points in the boundary region $R1'$ to $R0'$ (see Figs. 3 and 5): $t_{1 \rightarrow 0}(s_{\text{init}}) = t_L^+, t_R^-$, or t_G , where $s_{\text{init}} \in R1'$. Similarly, for jumps from the points in the boundary region $R0'$ to $R1'$ ($s_{\text{init}} \in R0'$) we

define $t_{0 \rightarrow 1}(s_{\text{init}}) = t_L^-, t_R^+,$ or t_G^+ . From the detailed balance condition we have that

$$t_{1 \rightarrow 0}(s) P_{\text{eq}}(s) = t_{0 \rightarrow 1}(s') P_{\text{eq}}(s'), \quad (35)$$

where s and s' are points in region $\mathbb{R}1'$ and $\mathbb{R}0'$ which are connected by the transfer matrix. For the survival time density we then choose the distribution of initial points proportional to the stationary influx from region $\mathbb{R}0'$. Furthermore, using the detailed balance condition and normalizing we have for the initial distribution in the $I=1$ state

$$f(s_{\text{init}}) = \frac{t_{1 \rightarrow 0}(s_{\text{init}}) P_{\text{eq}}(s_{\text{init}})}{\sum_{s_{\text{init}}} t_{1 \rightarrow 0}(s_{\text{init}}) P_{\text{eq}}(s_{\text{init}})}. \quad (36)$$

Similarly for the initial distribution in the $I=0$ state:

$$f(s_{\text{init}}) = \frac{t_{0 \rightarrow 1}(s_{\text{init}}) P_{\text{eq}}(s_{\text{init}})}{\sum_{s_{\text{init}}} t_{0 \rightarrow 1}(s_{\text{init}}) P_{\text{eq}}(s_{\text{init}})}, \quad (37)$$

which, together with Eqs. (32a), (32b), and (33), determine $\psi(t)$ and $\phi(t)$. We proceed to show the choices above for $f(s_{\text{init}})$ which satisfy ergodicity requirements.

Ergodicity requires that the ratio of times spent in the $I=1$ and $I=0$ state equals

$$R_{\text{eq}} = \frac{\sum_{s \in \mathbb{R}1} P_{\text{eq}}(s)}{\sum_{s \in \mathbb{R}0} P_{\text{eq}}(s)}. \quad (38)$$

From Eq. (32b) we have that the mean survival time can be written according to

$$\tau_{\text{surv}} = \int_0^\infty t \phi(t) dt = \sum_p (\bar{\eta}_p)^{-1} \bar{c}_p, \quad (39)$$

and identically for the mean waiting time τ_{wait} . We proceed by noticing that the eigenvalue equation (34) can be written as

$$\sum_{\tilde{s}} (\mathcal{W}^{\text{refl}}(s, \tilde{s}) - \mathcal{W}^{\text{abs}}(s, \tilde{s})) \bar{Q}_p(\tilde{s}) = -\bar{\eta}_p \bar{Q}_p(s), \quad (40)$$

where

$$\mathcal{W}^{\text{abs}}(s, \tilde{s}) = t_{1 \rightarrow 0}(s) \delta_{s, \tilde{s}} \delta_{s, s_{\text{init}}}, \quad (41)$$

with $s_{\text{init}} \in \mathbb{R}1'$, and $\mathcal{W}^{\text{refl}}(s, \tilde{s})$ satisfy $\sum_s \mathcal{W}^{\text{refl}}(s, \tilde{s}) = 0$. Summing Eq. (34) over s and using the above identity we obtain

$$\sum_s \bar{Q}_p(s) = \sum_{s_{\text{init}}} \bar{\eta}_p^{-1} t_{1 \rightarrow 0}(s_{\text{init}}) \bar{Q}_p(s_{\text{init}}) \quad (42)$$

which is a useful connection between quantities in the bulk ($s \in \mathbb{R}1$) and at the boundary $s_{\text{init}} \in \mathbb{R}1'$. Applying this relation to the expressions for the survival time, Eqs. (33), (36), and (39), and, we find

$$\tau_{\text{surv}} = \frac{\sum_p \sum_s \bar{Q}_p(s) \bar{Q}_p(\tilde{s})}{\sum_{s_{\text{init}}} t_{1 \rightarrow 0}(s_{\text{init}}) P_{\text{eq}}(s_{\text{init}})}. \quad (43)$$

Finally, from the completeness relation [37]

$$\sum_p \frac{\bar{Q}_p(s) \bar{Q}_p(\tilde{s})}{P_{\text{eq}}(\tilde{s})} = \delta_{s, \tilde{s}}, \quad (44)$$

we see that

$$\tau_{\text{surv}} = \frac{\sum_{s \in \mathbb{R}1} P_{\text{eq}}(s)}{\sum_{s_{\text{init}}} t_{1 \rightarrow 0}(s) P_{\text{eq}}(s_{\text{init}})}. \quad (45)$$

In a similar fashion

$$\tau_{\text{wait}} = \frac{\sum_{s \in \mathbb{R}0} P_{\text{eq}}(s)}{\sum_{s_{\text{init}}} t_{0 \rightarrow 1}(s) P_{\text{eq}}(s_{\text{init}})}, \quad (46)$$

which, via the detailed balance condition (35), shows that $\tau_{\text{surv}}/\tau_{\text{wait}} = R_{\text{eq}}$.

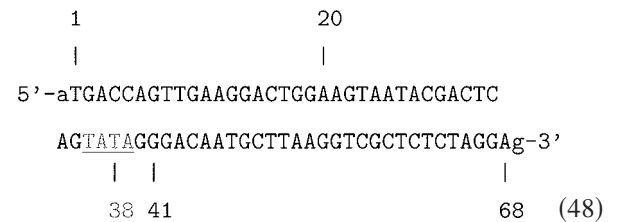
With the completeness relation (44) and Eq. (42) we find from Eqs. (33), (36), and (37), that \bar{c}_p can be written

$$\bar{c}_p = \frac{\bar{\eta}_p \left[\sum_s \bar{Q}_p(s) \right]^2}{\sum_p \bar{\eta}_p \left[\sum_s \bar{Q}_p(s) \right]^2}, \quad (47)$$

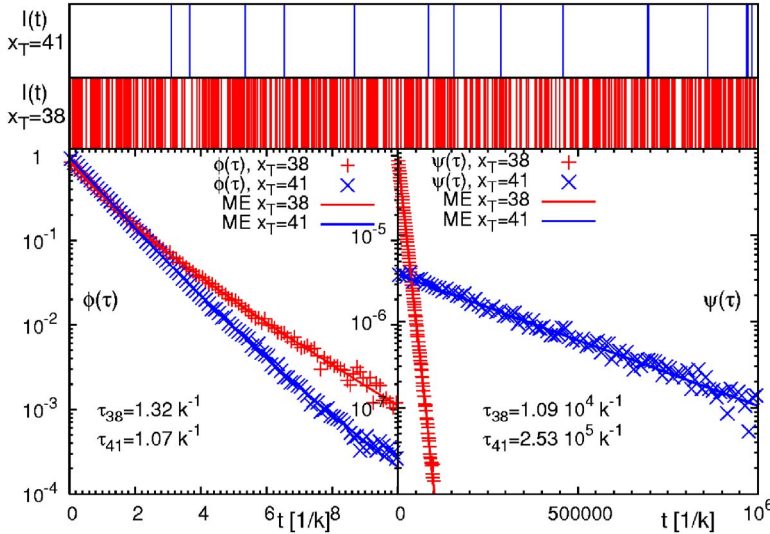
which is the form given in Eq. (22c).

C. Application to a viral promoter sequence

We show in Fig. 6 the time series obtained from a stochastic simulation (see the Appendix for a short introduction, and refer to Ref. [29] for details) for two different tag positions in the T7 bacteriophage promoter sequence



whose TATA motif is underlined [41]. A promoter is a sequence (often containing the so-called TATA motif) placed at the start of a gene, to which RNA polymerase is then recruited to initiate transcription [5]. Motives such as TATA are believed to assist polymerase during the transcription initiation [17,18]. Figure 6 shows the signal $I(t)$ at 37 °C for the tag positions $x_T = 38$ in the core of TATA, and $x_T = 41$ at the second GC bp after TATA. Bubble events occur much more frequently in TATA (the TA/AT stacking interaction is particularly weak [11]). This is quantified by the den-



sity of waiting times $\psi(\tau)$ spent in the $I=0$ state, whose characteristic time scale $\tau' = \int_0^\infty d\tau \tau \psi(\tau)$ is more than an order of magnitude longer than at $x_T=41$. In contrast, we observe similar behavior for the density of opening times $\phi(\tau)$ for $x_T=38$ and 41. The solid lines are the results from the master equation, see Sec. III B, showing excellent agreement with the Gillespie results. Notice that whereas $\psi(t)$ is characterized by a single exponential, $\phi(t)$ shows a crossover between different regimes. For long times both $\psi(t)$ and $\phi(t)$ decay exponentially as it should for a finite DNA stretch. This analysis shows that our derivation of the waiting time and survival time densities from the master equation is fully consistent with the result sampled from the time series of the Gillespie scheme.

V. REDUCED ONE-VARIABLE SCHEME FOR A HOMOPOLYMER

After addressing the derivation of the probability densities $\psi(t)$ and $\phi(t)$, and the details concerning the transfer matrix \mathcal{W} , we show how the master equation formalism reduces when a homopolymer sequence is considered, that is, a sequence with only one type of bps such as $(AT)_N$. Homopolymers can be realized experimentally. In the case that they are clamped, possible secondary structure formation does not appear to occur within the time scale which the bubbles remain open [16], and our formalism remains valid. In the case of long homopolymers, imperfect matching conditions apply, and additional degrees of freedom emerge [3]. Although this can be straightforwardly included in the formalism, we do not consider this case here.

In the homopolymer case, it is possible to obtain analytical results. To that end we note that for a homopolymer, all bps have the same statistical weights $u_{st}(x)$ and $u_{hb}(x)$. Formally, we therefore use $u=u_{st}u_{hb}$ for disruption of additional bps after bubble initiation. Due to this choice, we need to utilize the initiation factor σ_0 instead of the ring factor ξ , as σ_0 takes care of the fact that upon initiation two stacking bonds are broken [11,12,42]. If we furthermore assume that we are below the melting temperature $u < 1$, have a long

FIG. 6. (Color online) Top: Fluorescence time series $I(t)$ for the T7 promoter sequence, with tag positions $x_T=41$ (first panel) and $x_T=38$ (second panel), and $\Delta=0$. Bottom: Waiting time $[\psi(\tau)]$ and fluorescence survival time $[\phi(\tau)]$ densities, in units of k . The data points are results from the Gillespie algorithm, while the lines represent the numeric results obtained from the master equation (ME). All results are for $T=37$ $^\circ\text{C}$ and 100 mM NaCl with DNA parameters from [11].

DNA region $M \gg 1$, and consider bubbles far from the clamping, end effects are much less pronounced. It then follows that $P(x_L, m, t; x'_L, m') = \tilde{P}(m, t; m')$, and the master equation reduces to

$$\frac{\partial}{\partial t} \tilde{P}(m, t) = \tilde{\Gamma}^+(m-1) \tilde{P}(m-1, t) + \tilde{\Gamma}^-(m+1) \tilde{P}(m+1, t) - [\tilde{\Gamma}^+(m) + \tilde{\Gamma}^-(m)] \tilde{P}(m, t), \quad (49)$$

with the shorthand notation $\tilde{P}(m, t) = \tilde{P}(m, t; m')$. The forward transfer coefficients in this limit are given by

$$\begin{aligned} \tilde{\Gamma}^+(m=0) &= k \sigma_0 u s(0), \\ \tilde{\Gamma}^+(m)|_{m \geq 1} &= k u s(m), \end{aligned} \quad (50)$$

where we have incorporated the fact that a bubble size increase can occur by the opening of a bp at either the left or the right fork. For the backward transfer coefficients, we find

$$\tilde{\Gamma}^-(m) = k. \quad (51)$$

The eigenvalue equation corresponding to Eq. (49) has the comparatively simple structure

$$\begin{aligned} \tilde{\Gamma}^+(m-1) \tilde{Q}_p(m-1) + \tilde{\Gamma}^-(m+1) \tilde{Q}_p(m+1) - [\tilde{\Gamma}^+(m) \\ + \tilde{\Gamma}^-(m)] \tilde{Q}_p(m) = -\tilde{\eta}_p \tilde{Q}_p(m), \end{aligned} \quad (52)$$

with eigenvalues $\tilde{\eta}_p$ and eigenvectors $\tilde{Q}_p(m)$ ($p=0, 1, \dots, M$). The equation above is identical to the one in Refs. [23,28], and thus our generalized formalism is consistent with previous homopolymer models [23,28]. We note that the equilibrium distribution becomes

$$\tilde{P}_{\text{eq}}(m) = \frac{\mathcal{Z}(m)}{\sum_{m=0}^M \mathcal{Z}(m)}, \quad (53)$$

where $\mathcal{Z}(m) = \sigma_0(1+m)^{-c} u^m$ with $\mathcal{Z}(0)=1$, see Eqs. (1) and (2).

The autocorrelation function is, as before, simply proportional to the joint probability of having $m \geq 1$ at time t and $m \geq 1$ at initial time $t=0$. Proceeding as previously, and assuming that initially the system is at equilibrium, $P(m, 0; m', 0) = \delta_{mm'} \tilde{P}_{\text{eq}}(m)$, we have

$$\tilde{A}(t) = \langle I(t)I(0) \rangle - (\langle I \rangle)^2 = \sum_{p \neq 0} (\tilde{T}_p)^2 \exp\left(-\frac{t}{\tilde{\tau}_p}\right), \quad (54)$$

where $\tilde{T}_p = \sum_{m=1}^M \tilde{Q}_p(m)$. Here, we introduced the relaxation times $\tilde{\tau}_p \equiv 1/\tilde{\eta}_p$. As before, we write the correlation function according to $\tilde{A}(t) = \int d\tau \exp(-t/\tau) \tilde{f}(\tau)$, with the relaxation time spectrum

$$\tilde{f}(\tau) = \sum_{p \neq 0} (\tilde{T}_p)^2 \delta(\tau - \tilde{\tau}_p). \quad (55)$$

In Fig. 7, we compare the approximate result for $A(x_T, t)$ in the reduced one-variable homopolymer approach obtained by numerical solution of Eqs. (52) and using Eq. (54), with the general result from the master equation in Sec. III. We also show the corresponding weighted spectral densities given by Eq. (55). We note that the approximate expression works well only for the case of internal tagging and temperatures below the melting temperature (and for a sufficiently long DNA region); for a short DNA sequence, close-to-end-tagging or high temperatures (i.e., large bubbles) end effects, which are not included in the approximate model above, are significant.

In the analysis of Refs. [18,28] it was found that close to the melting transition at T_m , the mean correlation function takes its maximum (critical slowing down). In order to get an understanding of this behavior we here analytically obtain the largest relaxation time from the homopolymer model above. From Ref. [22] we have that the eigenvalues, see Eq. (52), are for $c=0$

$$\tilde{\eta}_p = k(u + 1 - 2u^{1/2} \cos \omega_p), \quad (56)$$

where ω_p ($0 < \omega_p \leq \pi$) is obtained from the transcendental equation

$$g(\omega_p) = \sin[(M+1)\omega_p] - \delta \sin[M\omega_p] = 0 \quad (57)$$

with $\delta = (1 - \sigma_0)u^{1/2}$. For $u \rightarrow 1$ and $\sigma_0 \rightarrow 0$ we get

$$\begin{aligned} g(\omega_p) &= \sin[(M+1)\omega_p] - \sin[M\omega_p] \\ &= 2 \sin \frac{\omega_p}{2} \cos \left[\left(M + \frac{1}{2} \right) \omega_p \right] \end{aligned} \quad (58)$$

so that we have

$$\omega_p = \frac{(p-1/2)\pi}{M+1/2} \quad (59)$$

which together with Eq. (56) give the eigenvalues. The smallest eigenvalue (largest relaxation time) is obtained for $p=1$, i.e., $\tilde{\eta}_1 = 2k\{1 - \cos(\pi/[2M+1])\} \approx k\pi^2/(2M+1)^2$ for $M \gg 1$, and therefore the largest relaxation time becomes

$$\tilde{\tau}_1 = \frac{1}{\tilde{\eta}_1} \approx \frac{(2M+1)^2}{\pi^2} k^{-1}. \quad (60)$$

We notice that the longest relaxation time scales as $\sim M^2$ at melting, in agreement with the findings in [26]. Figure 8 demonstrates the good agreement of the homopolymer result (τ_{\max} , 1D in the figure) with the maxima of the correlation time that coincide with the melting concentration.

VI. CONCLUSIONS

In this study we considered the bubble breathing dynamics in a heteropolymer DNA region characterized by statistical weights $u_{\text{st}}(x)$ for disrupting a stacking interaction between neighboring bps, and the weight $u_{\text{hb}}(x)$ for breaking a Watson-Crick hydrogen bond (x labels different bps), as well as the bubble initiation parameter (the ring-factor) σ_0 (ξ). For that purpose, we introduced a (2+1)-variable master equation governing the time evolution of the probability distribution to find a bubble of size m with left fork position x_L at time t , as well as a complementary Gillespie scheme. For the master equation, we present explicit forms for the transfer matrix \mathcal{W} , using a counting variable s instead of the left zipper fork position x_L and the bubble size m . We develop a formalism to derive the distribution of bubble lifetimes and the waiting times between subsequent bubble events. The time averages from the stochastic simulation agree well with the ensemble properties derived from the ME. We calculate the spectrum of relaxation times, and in particular the experimentally measurable autocorrelation function of a tagged bp is obtained. For the case of a long homopolymer DNA region with internal tagging and below the melting temperature the position of the bubble becomes irrelevant, and the master equation reduces to previous (1+1)-variable approaches in terms of the bubble size. We note that all parameters in our model are known from recent equilibrium measurements available for a wide range of temperatures and NaCl concentrations, except for the rate constant k for zipping that is the only free fit parameter. A better understanding of the zipping rate k remains an open question, requiring a detailed microscopic modeling of DNA breathing. It is expected that dynamic single molecule experiments of DNA bubble dynamics will provide significant new quantitative information on the DNA breathing, to aid in this development.

ACKNOWLEDGMENTS

We thank Maxim Frank-Kamenetskii, Oleg Krichevsky, and Kim Splittorff for very helpful discussions. S.K.B. acknowledges support from Virginia Tech. T.A. acknowledges partial support from the Knut and Alice Wallenberg Foundation. R.M. acknowledges partial funding from the Natural Sciences and Engineering Research Council (NSERC) of Canada and the Canada Research Chairs program.

APPENDIX: GILLESPIE APPROACH

In this section we briefly review the Gillespie algorithm. Together with the explicit expressions for the transfer coef-

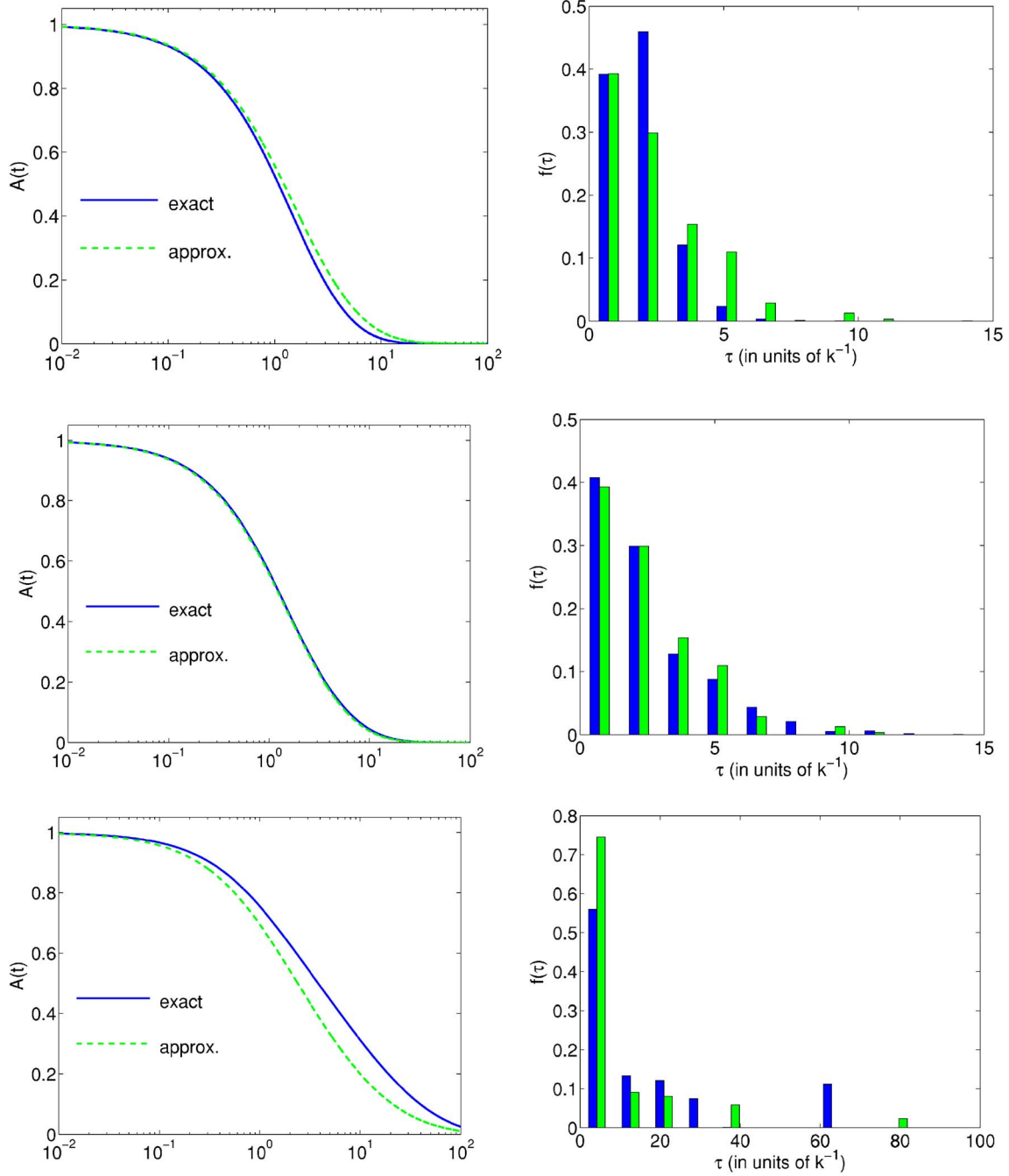


FIG. 7. (Color online) Autocorrelation $A(t)$ and spectral density $f(\tau)$ for a tagged bp in a homopolymer region: $u=u_{\text{hb}}u_{\text{st}}$. Top: Close-to-end-tagging far from T_m ($x_T=2$, $u=0.6$). Middle: Center-tagging far from T_m ($x_T=20$, $u=0.6$). Bottom: Center-tagging close to T_m ($x_T=20$, $u=0.9$). In the $A(t)$ plots the full lines (blue online) are the exact result. The dashed (green online) curves are approximated from Eqs. (52) and (54). In the spectral density plot the data were collected into ten bins. The light (green online) bars are the approximate one-variable results, Eq. (55), and the dark (blue online) bars are the exact result. The length of the DNA segment was $M=40$. The approximate expression only works well for internal tagging and below T_m .

ficients introduced in the previous section it is used to generate stochastic time series of bubble breathing. In particular we show how the motion of a tagged bp is obtained.

To denote a bubble state of m broken bps at position x_L we define the occupation number $b(x_L, m)$ for each lattice point in Fig. 3 with the properties $b(x_L, m)=1$ if the particular state $\{x_L, m\}$ is occupied, and $b(x_L, m)=0$ for unoccupied

states. For the completely zipped state $m=0$ there is no dependence on x_L , and we introduce the occupation number $b(0)$. The stochastic DNA breathing then corresponds to the nearest neighbor jump processes in the triangular lattice in Fig. 3. Each jump away from the state $\{x_L, m\}$ [i.e., from the state with $b(x_L, m)=1$] occurs at a random time τ and in a random “direction” to one of the nearest neighbors; it is gov-

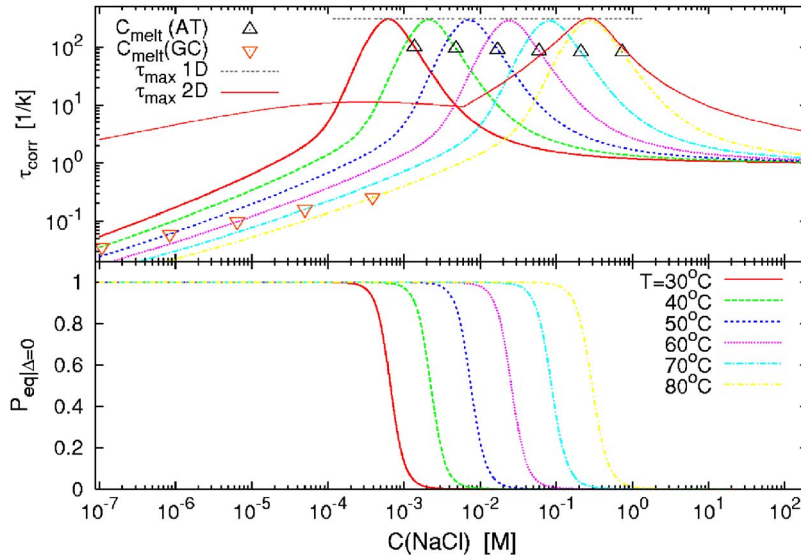


FIG. 8. (Color online) Top: Mean correlation time $\tau_{\text{corr}} = \int_0^\infty dt' A(t')/A(0)$ vs NaCl concentration for various temperatures T for the AT9 construct of Ref. [16], showing a critical slowing down at the melting concentration (compare lower panel). The triangles denote the melting concentration for infinitely long random AT and GC stretches. The curve denoted by $\tau_{\text{max}} 1D$ is the result given in Eq. (60), and $\tau_{\text{max}} 2D = \max\{\tau_p\}$, $p=1, \dots, S$ is the maximum relaxation time of the full problem specified in Sec. 3. Bottom: Opening probability of bp x_T .

erned by the reaction probability density function [43,44]

$$P(\tau, \mu, \nu) = t_\nu^\mu(x_L, m) \exp\left(-\tau \sum_{\mu, \nu} t_\nu^\mu(x_L, m)\right), \quad (\text{A1})$$

which for a given state (x_L, m) defines after what waiting time τ the next step occurs and in what “direction,” $\nu \in \{G, L, R\}$, $\mu \in \{+/-\}$. A simulation run produces a time series of occupied states $\{x_L, m\}$ and how long time $\tau = \tau_j$ ($j=1, \dots, N$, where N is the number of steps in the simulation) this particular state is occupied. This waiting time τ according to Eq. (A1) follows a Poisson distribution [45].

1. Tagged bp survival and waiting time densities

The stochastic variable $I(t)$ is then obtained by summing the Gillespie occupation number $b(x_L, m)$ [$b(x_L, m)$ takes only values 0 or 1] over region \mathbb{R}_1 , i.e.,

$$I(t) = \sum_{x_L, m \in \mathbb{R}_1} b(x_L, m). \quad (\text{A2})$$

From the sampled time series for $I(t)$ one can, for instance, calculate the waiting time distribution $\psi(\tau)$ of time spent in the $I=0$ state, as well as the survival time distribution $\phi(\tau)$ of times in the $I=1$ state. Explicit examples for $\psi(\tau)$ and $\phi(\tau)$ are shown in Sec. IV.

The probability that the tagged bp is open becomes

$$P_G(t_j) = \frac{1}{t_N} \sum_{j=1}^N \tau_j I(t_j), \quad (\text{A3})$$

where $t_j = \sum_{j'=1}^j \tau_{j'}$. For long times the explicit construction of the Gillespie scheme together with the detailed balance conditions guarantee that $P_G(t_j)$ tends to the equilibrium probability, i.e., that $P_G(t_j \rightarrow \infty) = \sum_{x_L, m \in \mathbb{R}_1} P^{\text{eq}}(x_L, m)$, where $P^{\text{eq}}(x_L, m)$ is given in Eq. (2).

2. Tagged base-pair autocorrelation function

The autocorrelation function for a tagged bp is obtained through

$$A_t(x_T, t) = \overline{I(t)I(0)} - [\overline{I(t)}]^2 = \frac{1}{T} \int_0^T I(t+t')I(t')dt' - \left(\frac{1}{T} \int_0^T I(t')dt' \right)^2, \quad (\text{A4})$$

where the overbar indicates a time average. For long times, by ergodicity $A_t(x_T, t)$ converges to the ensemble average, Eq. (14), from the master equation. The function $A_t(x_T, t)$ corresponds to the blinking autocorrelation function obtained in the FCS experiment from Ref. [16].

-
- [1] A. Kornberg, *DNA Synthesis* (W. H. Freeman, San Francisco, CA, 1974).
[2] C. R. Cantor and P. R. Schimmel, *Biophysical Chemistry, Part 3* (W. H. Freeman, New York, 1980).
[3] D. Poland and H. A. Scheraga, *Theory of Helix-Coil Transitions in Biopolymers* (Academic Press, New York, 1970).
[4] R. M. Wartell and A. S. Benight, Phys. Rep. **126**, 67 (1985).
[5] B. Alberts, A. Johnson, J. Lewis, M. Raff, K. Roberts, and P. Walter, *Molecular Biology of the Cell* (Garland, New York, 2002).
[6] S. B. Smith, Y. J. Cui, and C. Bustamante, Science **271**, 795 (1996).
[7] I. Rouzina and V. A. Bloomfield, Biophys. J. **80**, 882 (2001); **80**, 894 (2001).
[8] R. Metzler, T. Ambjörnsson, A. Hanke, Y. Zhang, and S. Levene, e-print physics/0609139, J. Comput. Theor. Nanosci. **4**, 1 (2007);
[9] M. D. Frank-Kamenetskii, *Unraveling DNA: The Most Impor-*

- tant Molecule of Life* (Perseus, Cambridge, MA, 1997).
- [10] Note that for $T=37$ °C we used that $1k_BT=0.62$ kcal/mol. Also note that writing Boltzmann factors for the free energies as $\exp(\beta\Delta G)$, with $\beta=1/(k_BT)$, a positive ΔG denotes an unstable bond.
- [11] A. Krueger, E. Protozanova, and M. D. Frank-Kamenetskii, *Biophys. J.* **90**, 3091 (2006).
- [12] R. D. Blake, J. W. Bizzaro, J. D. Blake, G. R. Day, S. G. Delcourt, J. Knowles, K. A. Marx, and J. SantaLucia, Jr., *Bioinformatics* **15**, 370 (1999).
- [13] R. Blossey and E. Carlon, *Phys. Rev. E* **68**, 061911 (2003).
- [14] E. Protozanova, P. Yakovchuk, and M. D. Frank-Kamenetskii, *J. Mol. Biol.* **342**, 775 (2004).
- [15] M. Guérion, M. Kochyan, and J.-L. Leroy, *Nature* (London) **328**, 89 (1987).
- [16] G. Altan-Bonnet, A. Libchaber, and O. Krichevsky, *Phys. Rev. Lett.* **90**, 138101 (2003).
- [17] C. H. Choi, G. Kalosakas, K. Ø. Ramsussen, M. Hiromura, A. R. Bishop, and A. Usheva, *Nucleic Acids Res.* **32**, 1584 (2004); G. Kalosakas, K. Ø. Ramsussen, A. R. Bishop, C. H. Choi, and A. Usheva, *Europhys. Lett.* **68**, 127 (2004).
- [18] T. Ambjörnsson, S. K. Banik, O. Krichevsky, and R. Metzler e-print q-bio.BM/0611090 (unpublished).
- [19] K. Pant, R. L. Karpel, and M. C. Williams, *J. Mol. Biol.* **327**, 571 (2003).
- [20] K. Pant, R. L. Karpel, I. Rouzina, and M. C. Williams, *J. Mol. Biol.* **336**, 851 (2004).
- [21] R. L. Karpel, *IUBMB Life* **53**, 161 (2002).
- [22] T. Ambjörnsson and R. Metzler, *Phys. Rev. E* **72**, 030901(R) (2005).
- [23] T. Ambjörnsson and R. Metzler, *J. Phys.: Condens. Matter* **17**, S1841 (2005).
- [24] A. Hanke and R. Metzler, *J. Phys. A* **36**, L473 (2003).
- [25] H. C. Fogedby and R. Metzler, *Phys. Rev. Lett.* **98**, 070601 (2007).
- [26] D. J. Bicout and E. Kats, *Phys. Rev. E* **70**, 010902(R) (2004).
- [27] e-print cond-mat/0610752, T. Novotny, J. N. Pedersen, M. S. Hansen, T. Ambjörnsson, and R. Metzler, *Europhys. Lett.* (to be published).
- [28] T. Ambjörnsson, S. K. Banik, O. Krichevsky, and R. Metzler, *Phys. Rev. Lett.* **97**, 128105 (2006).
- [29] S. K. Banik, T. Ambjörnsson, and R. Metzler, *Europhys. Lett.* **71**, 852 (2005).
- [30] T. Hwa, E. Marinari, K. Sneppen, and L. H. Tang, *Proc. Natl. Acad. Sci. U.S.A.* **100**, 4411 (2003).
- [31] M. Peyrard and A. R. Bishop, *Phys. Rev. Lett.* **62**, 2755 (1989); T. Dauxois, M. Peyrard, and A. R. Bishop, *Phys. Rev. E* **47**, R44 (1993); **47**, 684 (1993).
- [32] A. Campa and A. Giansanti, *Phys. Rev. E* **58**, 3585 (1998).
- [33] M. Fixman and J. J. Freire, *Biopolymers* **16**, 2693 (1977).
- [34] See C. Richard and A. J. Guttmann, *J. Stat. Phys.* **115**, 925 (2004), and references therein.
- [35] Also, $t_L^+(x_L=-1, m)=0$ and $t_R^-(x_L, m=M-x_L+1)=0$ for $m=2, \dots, M+1$ for completeness.
- [36] H. Risken, *The Fokker-Planck Equation* (Springer-Verlag, Berlin, 1989).
- [37] N. G. van Kampen, *Stochastic Processes in Physics and Chemistry*, 2nd Ed. (North-Holland, Amsterdam, 1992).
- [38] E. A. Di Marzio, C. M. Guttman, and J. D. Hoffman, *Faraday Discuss. R. Soc. Chem.* **68**, 210 (1979).
- [39] C. W. Gardiner, *Handbook of Stochastic Methods for Physics, Chemistry and the Natural Sciences* (Springer, Berlin, 1989).
- [40] T. Ambjörnsson, M. A. Lomholt, and R. Metzler, *J. Phys.: Condens. Matter* **17**, S3945 (2005).
- [41] G. Kalosakas, K. Ø. Rasmussen, A. R. Bishop, C. H. Choi, and A. Usheva, *Europhys. Lett.* **68**, 127 (2004).
- [42] J. SantaLucia, Jr., *Proc. Natl. Acad. Sci. U.S.A.* **95**, 1460 (1998).
- [43] D. T. Gillespie, *J. Comput. Phys.* **22**, 403 (1976).
- [44] D. T. Gillespie, *J. Phys. Chem.* **81**, 2340 (1977).
- [45] D. R. Cox, *Renewal Theory* (Wiley, New York, 1962).